



OPEN

Reduction of stress responses in honey bees by synthetic ligands targeting an allatostatin receptor

Adrià Sánchez-Morales², Véronique Gigoux³, Minos-Timotheos Matsoukas⁴, Laura Perez-Benito^{4,6}, Daniel Fourmy³, Ramón Alibes², Félix Busqué²✉, Arnau Cordoni^{4,5}✉ & Jean-Marc Devaud¹✉

Honey bees are of great economic and ecological importance, but are facing multiple stressors that can jeopardize their pollination efficiency and survival. Therefore, understanding the physiological bases of their stress response may help defining treatments to improve their resilience. We took an original approach to design molecules with this objective. We took advantage of the previous identified neuropeptide allatostatin A (ASTA) and its receptor (ASTA-R) as likely mediators of the honey bee response to a biologically relevant stressor, exposure to an alarm pheromone compound. A first series of ASTA-R ligands were identified through *in silico* screening using a homology 3D model of the receptor and *in vitro* binding experiments. One of these (A8) proved also efficient *in vivo*, as it could counteract two behavioral effects of pheromone exposure, albeit only in the millimolar range. This putative antagonist was used as a template for the chemical synthesis of a second generation of potential ligands. Among these, two compounds showed improved efficiency *in vivo* (in the micromolar range) as compared to A8 despite no major improvement in their affinity for the receptor *in vitro*. These new ligands are thus promising candidates for alleviating stress in honey bees.

Bees are vital to the survival of our ecosystem, by pollinating our crops, flowers and up to a third of all the food we eat¹. The number of wild bees has been on decline in recent years, and population losses observed by many beekeepers are due to exposure to multiple stressors². Thus, understanding physiological stress responses in this species, and identifying possible strategies to modulate them, is expected to open perspectives to improve their resilience^{2,3}.

Stress responses allow individuals to cope with adverse situations or stimuli through adapted physiological and behavioral outcomes, and are mediated by various neural and hormonal signals⁴. Although such responses have been mostly studied in mammals, a few studies have contributed to better characterizing potential stress signals in bees and other model invertebrate species. Among such signals are neuropeptides^{3,5–8}, a class of ubiquitous neuromodulators mediating neuroadaptive control of many organisms' internal state^{7–10}. As such, various neuropeptide receptors have been identified as potential therapeutic targets in humans^{10–12}, but might also be interesting for developing strategies to reduce stress and improve welfare in production animals.

A natural stressor to honey bees is the sting alarm pheromone (SAP), a complex mixture of odors released by bees facing a threat, and inducing the recruitment of nestmates to defend the colony¹³. In addition to increasing aggressiveness, SAP and its main component isopentylacetate (IPA) induce other behavioral and physiological responses which remind strongly of the vertebrate stress response: increased respiratory rate, reduced sensitivity to noxious stimuli ('analgesia'), decreased motivation for food, and learning impairment^{6,14–18}. Allatostatins are a family of invertebrate neuropeptides, three of which were identified in adult brain of honey bees (ASTA, ASTC, ASTCC), as well as their respective receptor. While the C receptor was shown to be targeted by two ligands (ASTC and ASTC CC), the A receptor is specific for ASTA, and shares sequence similarities with opioid

¹Centre de Recherches Sur La Cognition Animale (CRCA), Centre de Biologie Intégrative, 9 (CBI), Université de Toulouse, CNRS, Toulouse, France. ²Departament de Química, Universitat Autònoma de Barcelona, Bellaterra, 08193 Barcelona, Spain. ³Centre de Recherches en Cancérologie de Toulouse (CRCT), INSERM Unité Mixte de Recherche UMR-1037, CNRS Equipe de Recherche Labellisée ERL5294, Université de Toulouse, Toulouse, France. ⁴Unitat de Bioestadística, Universitat Autònoma de Barcelona, Bellaterra, 08193 Barcelona, Spain. ⁵Present address: Bioinformatics, ESCI-Universitat Pompeu Fabra, Passeig Pujades 1, 08003 Barcelona, Spain. ⁶Present address: Computational Chemistry, Janssen Research & Development, Janssen Pharmaceutica N. V., Turnhoutseweg 30, B-2340 Beerse, Belgium. ✉email: Felix.Busque@uab.cat; arnau.cordoni@esci.upf.edu; jean-marc.devaud@univ-tlse3.fr

and galanin receptors, its closest mammalian relatives⁶. Since injecting allatostatins in the micromolar range to unstressed bees mimics the learning impairment induced by IPA exposure, they can be considered as likely mediators of stress response^{6,19}. In *Drosophila*, ASTA also acts as a satiety signal that modulates food intake and maintenance of nutrient homeostasis, through the inhibition of food-research behavior^{20,21}. It participates into a more general action of promoting an energy-saving state through the coordination of feeding, digestion, locomotor activity and sleep, particularly under nutritional stress conditions²². Motivation for sugar is particularly sensitive to ASTA signaling: intake, acceptance, responsiveness and preference for this nutrient are reduced by ASTA^{20,21}. In addition, brain ASTA-expressing neurons also modulate sucrose-mediated appetitive learning in fruitflies²³. Interestingly, these biological functions are reminiscent of the capacity of both opioid and galanin signaling to modulate many aspects of stress response, including the reward system^{24,25}, leading to search for receptor agonists or antagonists with protective effects against stress in rodent systems (e.g.^{26–28}). Likewise, we asked whether synthetic ligands of allatostatin receptors could have similar actions. Here, we searched for ligands that might antagonize the activation of the A receptor by its ligand, ASTA, by combining *in silico* screening, binding assays and behavioral tests.

Methods

In silico screening of candidate molecules. A homology model of the honey bee allatostatin A receptor ASTA-R (NCBI: XP_006560262.1) was created using Modeller 9.12²⁹ based on the crystal structure of the antagonist-bound human δ -opioid receptor (PDB id 4N6H)³⁰. We constructed a pharmacophore model based on Electrostatic Maps (hydrophobic, hydrogen bond donor and hydrogen bond acceptor) as implemented in MOE 2013.08 (Molecular Operating Environment, Chemical Computing) which consisted in 13 pharmacophore features: 7 hydrophobic, 4 hydrogen bond acceptors and 2 hydrogen bond donors. Discovery Studio 3.5 software (Accelrys Software Inc., Discovery Studio Environment) was used for the virtual screening of ~5.5 million compounds from a filtered subset³¹ of the ZINC database³² using all pharmacophore models resulting from combinations of 5 to 7 pharmacophoric features out of the 13. To avoid steric clashes with the receptor, we used exclusion volumes derived from the receptor model. The fit value scoring was used to rank the compounds from best to worst fitting. Based on visual inspection, we selected 24 compounds from the best 1000 for experimental testing. Molecular dockings of the active compounds were performed with MOE 2016.08 using the Alpha Triangle method. The conformers were ranked by London dG scoring function to estimate the free energy of binding of the ligand from a given pose. Based on the dockings, we designed a scaffold for the next generation of ligands ('B' series).

Binding assays. A subset of compounds selected from the screening were tested in a competition binding assay with ¹²⁵I-allatostatin A transfected with allatostatin A receptor. HEK293T cells were grown onto 60-mm diameter culture dishes for 24 h in Dulbecco's Modified Eagle's medium (DMEM) supplemented with 10% of fetal bovine serum (FBS), in a humidified atmosphere at 95% air and 5% CO₂. Cells were transfected using Lipofectamin 2000 (Invitrogen Life Technologies) following provider's instructions (1 μ g DNA/ 3 μ l Lipofectamin 2000). 24 h later, cells were transferred to 24-well plates and incubated for 24 h. Cells were incubated for 60 min at 37 °C in 0.5 ml DMEM containing 0.1% bovine serum albumin with 5 nM of high performance liquid chromatography-purified Allatostatin-Dy647 (NHSDY647-PEG1, Dyomics GmbH, Jena, Germany) or ¹²⁵I-Allatostatin in the presence or in the absence of increased concentrations of unlabeled antagonists or allatostatin. We used GRQPYSFGL-amide, the most abundant isoform of allatostatin A in the brain, which already proved effective both *in vitro* and *in vivo*⁶. Cells were washed twice with cold phosphate-buffered saline, pH 7.4, containing 2% bovine serum albumin and once with cold phosphate-buffered saline, pH 7.4. For binding studies using ¹²⁵I-Allatostatin, cell-associated radioligand was collected by cell lysis with 0.1 N NaOH and the radioactivity was directly counted in a gamma counter (Auto-Gamma, Packard). For binding studies using allatostatin-Dy647, cells were recovered, transferred to flow cytometer tubes and cell-associated fluorescence was determined using a BD FACSCalibur™ flow cytometer. IC₅₀ (concentration inhibiting half of specific binding) was calculated using the non-linear curve fitting software GraphPad Prism (San Diego, CA).

Synthesis of second-generation ligands. *General procedures.* The solvents, chemicals, and reagents were acquired with high quality without any need for further purification from various commercial chemical companies such as, Merck (Darmstadt, Germany), Scharlab (Sentmenat, Spain), Apollo Scientific (Cheshire, United Kingdom), Alfa Aesar (Kandel, Germany), and TCI (Zwijndrecht Belgium). Solvents were dried by distillation over the appropriate drying agents. All reactions were monitored by analytical thin-layer chromatography (TLC) using silica gel 60 precoated aluminum plates (0.20 mm thickness). Flash column chromatography was performed using silica gel Geduran® SI 60 (40–63 μ m). ¹H NMR and ¹³C NMR spectra were recorded at 250, 360, 400 MHz and 90, 100.6 MHz, respectively. ¹⁹F NMR spectra were recorded at 250 MHz (see Supplementary Material). Proton chemical shifts are reported in ppm (δ) (CDCl₃: δ 7.26, acetone-d₆: δ 2.05, DMSO-d₆: δ 2.50, CD₂Cl₂: δ 5.32). Carbon chemical shifts are reported in ppm (δ) (CDCl₃: δ 77.16, acetone-d₆: δ 29.84, DMSO-d₆: δ 39.52, CD₂Cl₂: δ 53.84). NMR signals were assigned with the help of HSQC, HMBC, DEPT135. Melting points were determined on hot stage and are uncorrected. HRMS were recorded using electrospray ionization (ESI).

(Benzylsulfanyl)acetic acid, 5a. A mixture of benzyl bromide (3.13 mL, 26.32 mmol), thioglycolic acid (1.84 mL, 26.32 mmol) in methanol (10 mL) was prepared. Then, a solution of sodium hydroxide (2.11 g, 52.64 mmol) in methanol (53 mL) was added slowly and the resulting mixture was stirred during 2 h. After this time, the solvent was removed in vacuum using a rotatory evaporator. The resulting white solid was dissolved in water (100 mL) and cleaned with AcOEt (2 \times 75 mL). The aqueous layer was acidified dropwise with a solution of 1 M HCl until

pH 3 and extracted with AcOEt (3 × 75 mL). The whole organic layers were rinsed with brine (100 mL). Finally, the solvent was evaporated under reduced pressure and the resulting solid was purified by hexane washings to furnish (benzylsulfanyl)acetic acid **5a** (2.87 g, 15.74 mmol, 60% yield) as a white solid. ¹H NMR (360 MHz, DMSO-*d*₆): δ 12.61 (s, 1H, -COOH), 7.35–7.24 (m, 5H, H-2^{II}, H-3^{II}, H-4^{II}), 3.80 (s, 2H, H-2), 3.11 (s, 2H, H-1^I). The spectroscopic data was consistent with the literature³³.

(Phenethylsulfanyl)acetic acid, **5b**. Compound **5b** was prepared as described for **5a** by using 1-bromo-2-phenylethane (3.28 mL, 24.02 mmol) and thioglycolic acid (2.00 mL, 28.79 mmol) in MeOH (10 mL), and a solution of NaOH (2.19 g, 54.78 mmol) in MeOH (40 mL). Yield **5b**: 87% (4.10 g, 20.91 mmol) as white solid. ¹H NMR (360 MHz, DMSO-*d*₆): δ 12.57 (s, 1H, -COOH), 7.31–7.18 (m, 5H, H-2^{II}, H-3^{II}, H-4^{II}), 3.26 (s, 2H, H-2), 2.83 (s, 4H, H-1^I, H-2^I). The spectroscopic data was consistent with the literature³³.

((3-Phenylpropyl)sulfanyl)acetic acid, **5c**. Compound **5c** was prepared as described for **5a** by using 1-bromo-3-phenylpropane (5.45 mL, 35.86 mmol), thioglycolic acid (3.00 mL, 43.18 mmol) in methanol (20 mL), and a solution of NaOH (3.31 g, 82.76) in MeOH (60 mL). Yield **5c**: 95% (7.18 g, 34.13 mmol) as a white solid. ¹H NMR (360 MHz, DMSO-*d*₆): δ 12.55 (s, 1H, -COOH), 7.30–7.16 (m, 5H, H-2^{II}, H-3^{II}, H-4^{II}), 3.23 (s, 2H, H-2), 2.65 (t, *J*_{1,2}I = 7.4 Hz, 2H, H-1^I), 2.58 (t, *J*_{1,2}I = 7.3 Hz, 2H, H-3^I), 1.82 (m, *J*_{2,1}I = *J*_{1,3}I = 7.5 Hz, 2H, H-2^I). The spectroscopic data was consistent with the literature³³.

1-(2-Nitro-4-(trifluoromethyl)phenyl)-1H-1,2,4-triazole, **2a**. To a solution of 1,2,4-triazole (2.04 g, 29.48 mmol) in DMF (3.6 mL) was added 4-chloro-3-nitrobenzotrifluoride (4.0 mL, 27.22 mmol) and was heated to 100–105 °C. Once reached that temperature, K₂CO₃ (6.40 g, 48.31 mmol) was added slowly and the mixture was stirred at 115 °C during 30 min. Then, it was cooled to room temperature and 20 mL of water was added. The reaction crude and was extracted with AcOEt (4 × 20 mL) and the combined extracts were cleaned with water (3 × 15 mL) and brine (15 mL). Finally, the organics were dried with anhydrous Na₂SO₄ filtered and concentrated under vacuum. An orange solid was obtained identified as 1-(2-nitro-4-(trifluoromethyl)phenyl)-1H-1,2,4-triazole, **2a** (3.21 g, 12.4 mmol, 94% yield). Mp = 67–69 °C (from CH₂Cl₂). ¹H NMR (360 MHz, CD₂Cl₂): δ 8.51 (s, 1H, H-5), 8.28 (s, 1H, H-3^I), 8.12 (s, 1H, H-3), 8.05 (d, *J*_{6,5}I = 7.2 Hz, 1H, H-5^I), 7.81 (d, *J*_{6,5}I = 7.2 Hz, 1H, H-6^I). ¹⁹F NMR (250 MHz, CDCl₃): δ 63.39 (s, -CF₃). ¹³C NMR (90 MHz, CD₂Cl₂): δ 153.9 (C₃), 144.4 (C₂I), 144.2 (C₅), 133.1 (C₁I), 132.4 (q, *J*_{4,F} = 34.2 Hz, C₄I), 130.9 (q, *J*_{5,F} = 4.5 Hz, C₅I), 128.0 (C₆I), 123.5 (q, *J*_{3,F} = 3.6 Hz, C₃I), 122.7 (q, *J*_{1,F} = 271.8 Hz, -CF₃). IR (ATR): 2999, 1543, 1363, 1322, 1184, 1135, 1036, 979, 841 cm⁻¹. HRMS (ESI⁺): calcd. for [C₉H₅F₃N₄O₂ + H]⁺: 259.0443, found [M + H]⁺ 259.0442.

1-(4-Methyl-2-nitrophenyl)-1H-1,2,4-triazole, **2b**. To a solution of 1,2,4-triazole (137 mg, 1.98 mmol) in DMF (0.25 mL) was added 4-chloro-3-nitrotoluene (0.24 mL, 1.80 mmol) and was heated to 105 °C. Once reached that temperature, K₂CO₃ (438 mg, 3.08 mmol) was added slowly and the mixture was heated to 115 °C and stirred for 6 h. Then, another portion of 1,2,4-triazole (130 mg, 1.88 mmol) and DMF (0.25 mL) was added and the mixture was stirred overnight. The crude was cooled to room temperature and poured into a beaker with water/ice (10 mL). The resulting suspension was extracted with EtOAc (3 × 15 mL) and cleaned with and brine (15 mL). Finally, the organic layers were dried with anhydrous Na₂SO₄, filtered and concentrated under vacuum. The resulting red oil was purified by column chromatography (EtOAc/hexane, 1:1) to obtain a yellow solid identified as 1-(4-methyl-2-nitrophenyl)-1H-1,2,4-triazole, **2b** (301 mg, 1.47 mmol, 82% yield). Mp = 67–69 °C (from CH₂Cl₂). ¹H NMR (400 MHz, CDCl₃): δ 8.36 (s, 1H, H-5), 8.09 (s, 1H, H-3), 7.83 (m, *J*_{5,4}I = 1.2 Hz, 1H, H-3^I), 7.54 (dm, *J*_{5,6}I = 8.1 Hz, *J*_{5,3}I = 1.2 Hz, 1H, H-5^I), 7.44 (d, *J*_{6,5}I = 8.1 Hz, 1H, H-6^I). ¹³C NMR (100 MHz, CDCl₃): δ 153.1 (C₃), 144.5 (C₂I), 144.0 (C₅), 141.7 (C₄I), 134.3 (C₅I), 127.9 (C₁I), 127.5 (C₆I), 125.9 (C₆I), 21.2 (-CH₃). IR (ATR): 3113, 1533, 1355, 1278, 1214, 1142, 1042, 985, 837 cm⁻¹. HRMS (ESI⁺): calcd. for [C₉H₈N₄O₂ + H]⁺: 205.0726, found [M + H]⁺ 205.0724.

2-(1H-1,2,4-triazol-1-yl)-5-(trifluoromethyl)aniline, **3a**. Compound **2a** (9.98 g, 38.65 mmol) and Na₂S (3.02 g, 38.6 mmol) were dissolved with a 1:1 degassed mixture of dioxane and water (140 mL) under N₂ atmosphere. The reaction mixture was heated to 75–80 °C and stirred over 2 h. Another portion of Na₂S (1.50 g, 19.25 mmol) was added and the mixture was stirred 1 h. Then, the reaction was quenched with a saturated aqueous solution of NaHCO₃ (15 mL) and the crude product was extracted with AcOEt (3 × 30 mL) and the combined organic layers were cleaned with water (3 × 20 mL) and brine (20 mL). Then, it was dried over anhydrous Na₂SO₄ and the solvent was removed under vacuum. The resulting orange oil was purified by column chromatography (AcOEt/hexane, 1:1 → 1:2) to furnish a yellow solid identified as 2-(1H-1,2,4-triazol-1-yl)-5-(trifluoromethyl)aniline, **3a** (4.48 g, 19.65 mmol, 51% yield). Mp = 122–123 °C (from CH₂Cl₂). ¹H NMR (360 MHz, CD₂Cl₂): δ 8.44 (s, 1H, H-5^I), 8.15 (s, 1H, H-3^I), 7.34 (d, *J*_{3,4} = 8.3 Hz, 1H, H-3), 7.13 (s, 1H, H-6), 7.04 (d, *J*_{4,3} = 8.3 Hz, 1H, H-4), 4.97 (s, 2H, -NH₂). ¹⁹F NMR (250 MHz, CDCl₃): δ 63.53 (s, -CF₃). ¹³C NMR (90 MHz, CD₂Cl₂): δ 153.1 (C₃I), 144.1 (C₅^I), 142.0 (C₁), 132.0 (q, *J*_{5,F} = 33.5 Hz, C₅), 125.3 (C₂), 125.0 (C₃), 124.3 (q, *J*_{1,F} = 270.5 Hz, -CF₃), 114.8 (q, *J*_{4,F} = 4.1 Hz, C₄), 114.6 (q, *J*_{6,F} = 3.5 Hz, C₆). IR (ATR): 3432, 3320, 1635, 1456, 1344, 1271, 1149, 1102, 958 cm⁻¹. HRMS (ESI⁺): calcd. for [C₉H₇F₃N₄ + H]⁺: 229.0701, found [M + H]⁺ 229.0701.

5-methyl-2-(1H-1,2,4-triazol-1-yl)aniline, **3b**. Compound **2b** (5.00 g, 24.49 mmol) and Na₂S (2.87 g, 36.77 mmol) were dissolved with a 1:1 degassed mixture of dioxane and water (100 mL) under N₂ atmosphere. The reaction mixture was heated to 75 °C and stirred over 1 h. Then, a second portion of Na₂S (956 mg, 12.25 mmols) was added and the mixture was stirred 1 h. The reaction was quenched with a saturated aqueous solution

of NaHCO₃ (15 mL) and the crude product was extracted with AcOEt (3 × 100 mL) and the combined organic layers were cleaned with water (2 × 150 mL) and brine (250 mL). Then, it was dried over anhydrous Na₂SO₄ and the solvent was removed under vacuum. The resulting yellow solid was purified by column chromatography (AcOEt/hexane, 2:1) to furnish a yellow solid identified as 5-methyl-2-(1*H*-1,2,4-triazol-1-yl)aniline 3b (2.91 g, 16.70 mmol, 60% yield). Mp = 67–69 °C (from CH₂Cl₂). ¹H NMR (400 MHz, CDCl₃): δ 8.31 (s, 1H, H-5^I), 8.12 (s, 1H, H-3^I), 7.05 (d, *J*_{3,4} = 8.0 Hz, 1H, H-3), 6.66 (s, 1H, H-6), 6.66 (d, *J*_{4,3} = 8.0 Hz, 1H, H-4), 4.41 (s, 2H, -NH₂), 2.30 (s, 3H, -CH₃). ¹³C NMR (100 MHz, CDCl₃): δ 152.4 (C₃I), 143.4 (C₅^I), 140.9 (C₁), 140.4 (C₅), 124.3 (C₃), 120.7 (C₂), 119.3 (C₄), 117.9 (C₆), 21.3 (-CH₃). IR (ATR): 3422, 3336, 3118, 1631, 1518, 1276, 1137, 956 cm⁻¹. HRMS (ESI⁺): calcd. for [C₉H₁₀N₄ + H]⁺: 175.0984, found [M + H]⁺ 175.0980.

N-(2-(1*H*-1,2,4-triazol-1-yl)-5-(trifluoromethyl)phenyl)-2-(benzylthio)acetamide, B1. To a solution of compound 5a (807 mg, 4.43 mmol), and DMF (4 drops) in dry CH₂Cl₂ (8 mL) under N₂ atmosphere, SOCl₂ (0.95 mL, 13.09 mmol) was added dropwise, and the mixture was heated to reflux conditions during 4 h. After that, the solvent was removed under reduced pressure and the crude was redissolved in dry CH₂Cl₂ (8 mL), and the corresponding solution concentrated again under reduced pressure. This operation was repeated 3 times in order to remove the traces of SOCl₂ and the obtained acyl chloride was dissolved in anhydrous ACN (10 mL) under N₂ atmosphere conditions. In another round bottom flask, DIPEA (0.77 mL, 4.42 mmol) was added to a solution of compound 3a (501 mg, 2.20 mmol) in dry ACN (10 mL) under N₂ atmosphere. This mixture was heated to the reflux temperature, and the acyl chloride solution was slowly added in small portions (1.5 mL) every 15 min. Next, the mixture was let stirred overnight at room temperature. The reaction was quenched with water (30 mL) and diluted with CH₂Cl₂ (30 mL). The organic layer was separated and cleaned with water (2 × 30 mL) and brine (30 mL), dried with anhydrous Na₂SO₄ and removed under vacuum. The brown oil obtained was purified by column chromatography (CH₂Cl₂/Et₂O, 2:1) to furnish a pale brown solid identified as *N*-(2-(1*H*-1,2,4-triazol-1-yl)-5-(trifluoromethyl)phenyl)-2-(benzylthio)acetamide, B1 (713 mg, 1.82 mmol, 83% yield). Mp = 104–107 °C (from CH₂Cl₂). ¹H NMR (360 MHz, CD₂Cl₂): δ 10.51 (s, 1H, -HNCO-), 8.82 (s, 1H, H-6^{III}), 8.53 (s, 1H, H-5^{IV}), 8.24 (s, 1H, H-3^{IV}), 7.52 (m, *J*_{3III,4III} = 8.3 Hz, 1H, H-3^{III}), 7.50 (m, *J*_{4III,3III} = 8.3 Hz, 1H, H-4^{III}), 7.28–7.16 (m, 5H, 2xH-2^{II}, 2xH-3^{II}, H-4^{II}), 3.72 (s, 2H, H-1^I), 3.27 (s, 2H, H-2). ¹⁹F NMR (250 MHz, CDCl₃): δ 63.30 (s, -CF₃). ¹³C NMR (90.5 MHz, CD₂Cl₂): δ 168.1 (C₁), 153.6 (C₃IV), 144.3 (C₅IV), 137.2 (C₁II), 132.6 (C₁II), 131.5 (q, *J*_{5III,F} = 32.5 Hz, C₅III), 129.4 (C₂II), 128.9 (C₃II), 128.7 (C₂III), 127.7 (C₄II), 123.9 (q, *J*_{1IV,F} = 270.9 Hz, C₁IV), 123.9 (C₃III), 121.4 (q, *J*_{4III,F} = 3.9 Hz, C₄III), 120.2 (q, *J*_{6III,F} = 4.1 Hz, C₆III), 37.4 (C₁I), 37.0 (C₂). IR (ATR): 3286, 1687, 1531, 1476, 1435, 1330, 1132 cm⁻¹. HRMS (ESI⁺): calcd. for [C₁₈H₁₅F₃N₄OS + H]⁺: 393.0997, found [M + H]⁺ 393.0991.

N-(2-(1*H*-1,2,4-triazol-1-yl)-5-(trifluoromethyl)phenyl)-2-(phenethylthio)acetamide, B2. Compound B2 was prepared as described for B1 by using compound 5b (739 mg, 3.94 mmol), SOCl₂ (0.93 mL, 12.86 mmol) and DMF (5 drops) in dry CH₂Cl₂ (7 mL). The resulting acyl chloride was dissolved in dry ACN (10 mL) and was added to a solution of compound 3a (224 mg, 0.98 mmol), DIPEA (0.35 mL, 2.04 mmol) in dry ACN (5 mL). Yield B2: 60% (238 mg, 0.59 mmol) as pale-yellow solid. Mp = 70–72 °C (from CH₂Cl₂). ¹H NMR (400 MHz, CD₂Cl₂): δ 10.60 (s, 1H, -HNCO-), 8.89 (s, 1H, H-6^{III}), 8.51 (s, 1H, H-5^{IV}), 8.22 (s, 1H, H-3^{IV}), 7.55 (m, *J*_{3III,4III} = 8.4 Hz, 1H, H-3^{III}), 7.51 (m, *J*_{4III,3III} = 8.5 Hz, 1H, H-4^{III}), 7.30–7.17 (m, 5H, 2xH-2^{II}, 2xH-3^{II}, H-4^{II}), 3.37 (s, 2H, H-2), 2.86 (s, 2H, H-2^I), 2.77 (s, 2H, H-1^I). ¹⁹F NMR (250 MHz, CDCl₃): δ 63.29 (s, -CF₃). ¹³C NMR (100.6 MHz, CD₂Cl₂): δ 168.5 (C₁), 153.8 (C₃IV), 144.4 (C₅IV), 140.4 (C₁II), 132.9 (C₁III), 131.8 (q, *J*_{5III,F} = 33.2 Hz, C₅III), 129.0 (5C, C₂III, 2xC₂II, 2xC₃II), 127.0 (C₄II), 124.3 (C₃III), 124.1 (q, *J*_{1IV,F} = 273.0 Hz, C₁IV), 121.6 (q, *J*_{4III,F} = 4.1 Hz, C₄III), 120.4 (q, *J*_{6III,F} = 4.1 Hz, C₆III), 37.9 (C₂), 36.0 (C₂I), 34.8 (C₁I). IR (ATR): 3275, 1687, 1536, 1479, 1434, 1333, 1124 cm⁻¹. HRMS (ESI⁺): calcd. for [C₁₉H₁₇F₃N₄OS + H]⁺: 407.1153, found [M + H]⁺ 407.1151.

N-(2-(1*H*-1,2,4-triazol-1-yl)-5-(trifluoromethyl)phenyl)-2-((3-phenylpropyl)thio)acetamide, B3. Compound B3 was prepared as described for B1 by using compound 5c (832 mg, 3.95 mmol), SOCl₂ (0.75 mL, 10.38 mmol) and DMF (5 drops) in dry CH₂Cl₂ (8 mL). The resulting acyl chloride was dissolved in dry ACN (10 mL) and was added to a solution of compound 3a (448 mg, 1.96 mmol), DIPEA (1 mL, 5.74 mmol) in dry ACN (10 mL). Yield B3: 56% (463 mg, 1.10 mmol) as a pale-yellow solid. Mp = 78–80 °C (from CH₂Cl₂). ¹H NMR (400 MHz, CD₂Cl₂): δ 10.60 (s, 1H, -HNCO-), 8.87 (s, 1H, H-6^{III}), 8.48 (s, 1H, H-5^{IV}), 8.24 (s, 1H, H-3^{IV}), 7.55 (m, *J*_{3III,4III} = 8.4 Hz, 1H, H-3^{III}), 7.52 (m, *J*_{4III,3III} = 8.5 Hz, *J*_{4III,6III} = 1.8 Hz, 1H, H-4^{III}), 7.26–7.13 (m, 5H, 2xH-2^{II}, 2xH-3^{II}, H-4^{II}), 3.37 (s, 2H, H-2), 2.66 (m, *J*_{1,2I} = 7.4 Hz, 2H, H-3^I), 2.51 (m, *J*_{1,2I} = 7.6 Hz, 2H, H-1^I), 1.86 (m, *J*_{2,1I,3I} = 7.6 Hz, 2H, H-2^I). ¹⁹F NMR (250 MHz, CDCl₃): δ 63.27 (s, -CF₃). ¹³C NMR (100.6 MHz, CD₂Cl₂): δ 168.7 (C₁), 153.8 (C₃IV), 144.4 (C₅IV), 141.8 (C₁II), 132.9 (C₂III), 131.8 (q, *J*_{5III,F} = 32.9 Hz, C₅III), 129.0 (C₁III), 128.9 (5C, 2xC₂II, 2xC₃II, C₄II), 124.3 (C₃III), 124.1 (q, *J*_{1IV,F} = 272.0 Hz, -CF₃), 121.6 (q, *J*_{4III,F} = 4.2 Hz, C₄III), 120.4 (q, *J*_{6III,F} = 4.2 Hz, C₆III), 37.8 (C₂), 35.0 (C₃I), 32.8 (C₁I), 31.1 (C₂I). IR (ATR): 3186, 1690, 1533, 1479, 1426, 1330, 1170, 1127 cm⁻¹. HRMS (ESI⁺): calcd. for [C₂₀H₁₉F₃N₄OS + H]⁺: 421.1310, found [M + H]⁺ 421.1308.

2-(benzylthio)-*N*-(5-methyl-2-(1*H*-1,2,4-triazol-1-yl)phenyl)acetamide, B4. To a solution of compound 5a (514 mg, 2.82 mmol) and HATU (1.049 g, 2.76 mmol) in anhydrous THF (16 mL) and anhydrous DMF (2 mL), DIPEA (1.5 mL, 7.6 mmol) was added under N₂ atmosphere and the mixture was stirred for 30 min. Then, another solution of amine 3b (307 mg, 1.76 mmol) in anhydrous THF (5 mL) under N₂ atmosphere was prepared and added to the previous solution. The reacting mixture was stirred overnight, quenched with water (20 mL) and extracted with CH₂Cl₂ (3 × 25 mL). The combined organic extracts were cleaned with brine (75 mL), dried with Na₂SO₄, filtered and concentrated under reduced pressure. The obtained brown oil was purified by column chro-

matography (EtOAc/hexane, 1:1) to furnish a white solid identified as 2-(benzylthio)-*N*-(5-methyl-2-(1*H*-1,2,4-triazol-1-yl)phenyl)acetamide, B4 (401 mg, 1.19 mmol, 60% yield). Mp = 104–106 °C (from CH₂Cl₂). ¹H NMR (400 MHz, acetone-*d*₆): δ 9.97 (s, 1H, -HNCO-), 8.79 (s, 1H, H-5^{IV}), 8.22 (s, 1H, H-6^{III}), 8.22 (s, 1H, H-3^{IV}), 7.47 (m, *J*_{III,4}III = 8.1 Hz, 1H, H-3^{III}), 7.29–7.19 (m, 5H, 2xH-2^{II}, 2xH-3^{II}, H-4^{II}), 7.11 (m, *J*_{III,3}III = 8.1 Hz, 1H, H-4^{III}), 3.75 (s, 2H, H-1^I), 3.26 (s, 2H, H-2), 2.41 (s, 3H, H-1^V). ¹³C NMR (100.6 MHz, acetone-*d*₆): δ 168.0 (C₁), 153.5 (C₃IV), 145.3 (C₅IV), 140.3 (C₅III), 138.4 (C₁II), 132.7 (C₁II), 129.9 (C₂II), 129.3 (C₃II), 127.9 (C₄II), 125.9 (C₄III), 125.0 (C₃III), 124.1 (C₆III), 37.0 (C₁I), 36.5 (C₂), 36.5 (-CH₃). IR (ATR): 3273, 1673, 1592, 1538, 1498, 1374, 1141 cm⁻¹. HRMS (ESI⁺): calcd. for [C₁₈H₁₈N₄OS + Na]⁺: 361.1099, found [M + Na]⁺ 361.1097.

N-(5-methyl-2-(1*H*-1,2,4-triazol-1-yl)phenyl)-2-(phenethylthio)acetamide, B5. Compound B5 was prepared as described for B4 by using a solution of compound 5b (518 mg, 2.64 mmol), HATU (1.00 g, 2.63 mmol) and DIPEA (1.2 mL, 6.9 mmol) in anhydrous THF (17 mL) and anhydrous DMF (2 mL). The activated acid solution was added to a solution of amine 3b (306 mg, 1.76 mmol) in dry THF (8 mL). Yield B5: 83% (514 mg, 1.46 mmol) as a white solid. Mp = 109–110 °C (from CH₂Cl₂). ¹H NMR (360 MHz, CD₂Cl₂): δ 10.07 (s, 1H, -HNCO-), 8.39 (s, 1H, H-5^{IV}), 8.26 (s, 1H, H-6^{III}), 8.15 (s, 1H, H-3^{IV}), 7.30–7.16 (m, 6H, H-3^{III}, 2xH-2^{II}, 2xH-3^{II}, H-4^{II}), 7.07 (m, *J*_{III,3}III = 8.1 Hz, 1H, H-4^{III}), 3.31 (s, 2H, H-2), 2.81 (s, 2H, H-2^I), 2.71 (s, 2H, H-1^I), 2.43 (s, 1H, -CH₃). ¹³C NMR (90.5 MHz, CD₂Cl₂): δ 168.0 (C₁), 153.3 (C₃IV), 144.3 (C₅IV), 140.8 (C₅II), 140.5 (C₁II), 132.1 (C₁III), 129.0 (4C, 2xC₂II, 2xC₃II), 126.9 (C₄II), 125.8 (C₃III), 124.8 (C₂III), 124.0 (C₄III), 123.8 (C₆III), 37.8 (C₂), 36.0 (C₂I), 34.8 (C₁I), 21.8 (-CH₃). IR (ATR): 3277, 1683, 1588, 1529, 1482, 1280 cm⁻¹. HRMS (ESI⁺): calcd. for [C₁₉H₂₀N₄OS + H]⁺: 353.1436 m/z [M + H]⁺; found 353.1433.

N-(5-methyl-2-(1*H*-1,2,4-triazol-1-yl)phenyl)-2-(phenylpropylthio)acetamide, B6. Compound B6 was prepared as described for B4 by using a solution of compound 5c (197 mg, 0.94 mmol), HATU (360 mg, 0.94 mmol) and DIPEA (0.44 mL, 2.50 mmol) in anhydrous THF (5 mL) and anhydrous DMF (1 mL). The activated acid solution was added to a solution of amine 3b (109 mg, 0.63 mmol) in dry THF (5 mL). Yield B6: 50% (120 mg, 0.31 mmol) as a white solid. Mp = 78–80 °C (from CH₂Cl₂). ¹H NMR (400 MHz, CD₂Cl₂): δ 10.06 (s, 1H, -HNCO-), 8.35 (s, 1H, H-5^{IV}), 8.24 (s, 1H, H-6^{III}), 8.16 (s, 1H, H-3^{IV}), 7.27–7.14 (m, 6H, H-3^{III}, 2xH-2^{II}, 2xH-3^{II}, H-4^{II}), 7.07 (m, *J*_{III,3}III = 8.2 Hz, *J*_{III,6}III = 1.2 Hz, 1H, H-4^{III}), 3.30 (s, 2H, H-2), 2.65 (m, *J*_{1,2}I = 7.5 Hz, 2H, H-3^I), 2.46 (m, *J*_{1,2}I = 7.6 Hz, 2H, H-1^I), 2.44 (s, 3H, H-1^V), 1.84 (m, *J*_{1,1}I₃I = 7.5 Hz, 2H, H-2^I). ¹³C NMR (100.6 MHz, CD₂Cl₂): δ 168.1 (C₁), 153.4 (C₃IV), 144.3 (C₅IV), 141.9 (C₁II), 140.8 (C₅III), 132.2 (C₁III), 129.0 (C₂II), 128.9 (C₂II), 126.5 (C₄II), 125.8 (C₄III), 124.9 (C₂III), 124.1 (C₃III), 123.9 (C₆III), 37.8 (C₂), 35.1 (C₃I), 32.8 (C₁I), 31.1 (C₂I), 21.8 (-CH₃). IR (ATR): 2946, 1688, 1593, 1542, 1509, 1414, 1283 cm⁻¹. HRMS (ESI⁺): calcd. for [C₂₀H₂₂N₄OS + H]⁺: 367.1593, found [M + H]⁺ 367.1591.

cAMP levels in culture medium. HEK293T cells (ATCC-CRL-11268, American-type culture collection, United States) were grown onto 60-mm diameter culture dishes for 24 h in Dulbecco's Modified Eagle's medium (DMEM) supplemented with 10% of fetal bovine serum (FBS), in a humidified atmosphere at 95% air and 5% CO₂. Cells were transfected using Lipofectamin 2000 (Invitrogen Life Technologies) following provider's instructions (1 μg DNA/3 μl Lipofectamin 2000). 24 h later, cells were transferred to 24-well plates at 150,000 cells/well and incubated for 24 h. Cells were incubated for 30 min at 37 °C with 10 μM forskolin in presence or absence of allatostatin and/or antagonist (B5 or B6) in 0.5 ml DMEM. The cells were then washed with phosphate-buffered saline and lysed. The intracellular levels of cyclic adenosine monophosphate (cAMP) were determined with a DetectX[®] Cyclic AMP (cAMP) Direct Immunoassay kit (K019-H1; Arbor Assays, Ann Arbor, MI, USA) according to the manufacturer instructions.

Behavioral assays. Honey bees (*Apis mellifera*, Buckfast) were collected daily from colonies at the experimental apiary (~30 hives) located on the campus of Toulouse University. They were taken from different colonies from one day to another, in order to take into account inter-colony variability (due to e.g. genetically different queens, colony size or health status). Experiments were conducted between May 2018 and July 2019. After collection, they were cold-anesthetized and mounted in restraining holders, then fed with 5 μL sucrose (50% in water) before proceeding. During resting periods between manipulations, they were kept in the dark at room temperature. All chemicals (except the treatment solutions) were purchased from Sigma (Lyon, France).

Assessment of learning performance. Bees were injected with A8 diluted in phosphate buffer saline (PBS, Sigma-Aldrich) or PBS alone for controls (200 nL in the head capsule), 1 h after feeding. One hour later, they were exposed for 15 min to isopentyl acetate (IPA, 24% in paraffin oil), and underwent a 3-trial olfactory conditioning 45 min later. Briefly, on each trial they were trained to associate an odorant (1-hexanol or 1-nonanol, presented for 4 s) with a sucrose reward (delivered for 3 s). Extension of the proboscis (mouthparts) during the odor presentation and before the reward delivery was counted as a conditioned response. Details of the protocol can be found elsewhere⁶. Bees not responding to sucrose alone were discarded.

Assessment of appetitive response. One hour after feeding, bees were injected with one of the treatment solutions (200 nL in the head capsule) then exposed to IPA (as above) 1 h later. The appetitive response was assessed 45 min after exposure (i.e. 3 h following feeding). For this, the proboscis extension reflex (PER) was tested in response to applying increasing sucrose concentrations (0.1, 0.3, 1, 3, 10, 30%) on the antennae, and the presence or absence of a full extension of the proboscis was noted for each concentration. Since sucrose was diluted in water, bees were allowed to drink water ad libitum before the test, and antennal applications of water were interspersed with sucrose presentations to ensure that the responses were specifically elicited by sucrose. All bees responding to water were discarded.

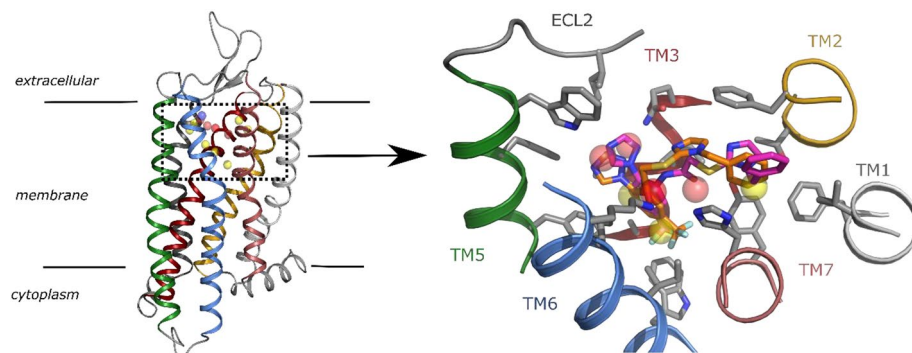


Figure 1. ASTA Receptor model and pharmacophore. (Left) Cartoon representation of the homology model of the ASTA-R with transmembrane helices displayed in different colors. The dotted rectangle indicates the localization of the typical orthosteric binding pocket in class A GPCRs (zoomed in the right panel). Spheres represent the 13 pharmacophoric features defined for the virtual screening (yellow: hydrophobic, red: hydrogen bond acceptor, purple: negative charge). (Right) Zoom of the orthosteric pocket of ASTA displaying the best two docking poses of compound A8 (colored by atom type with carbons in orange or magenta). Spheres represent the 7 pharmacophoric features matched by compound A8 in the virtual screening. Helices are shown as cartoon and residue side-chains around A8 as sticks (colored by atom type with carbons in grey). ECL: extracellular loop; TM: transmembrane helix.

Statistical analysis. Sample sizes are provided in the figure legends. Learning performance was measured, for each treatment group, as the percentage of bees displaying a conditioned response at the corresponding trial. The effect of treatment on learning performance was assessed using a one-factor ANOVA on the proportions of conditioned responses by the end of conditioning (3rd trial). Appetitive responses were analyzed in two ways. For each treatment, an individual sucrose responsiveness score (SRS, ranging between 0 and 6) was calculated as the sum of PER displayed over the 6 sucrose presentations. For each tested molecule, effects of molarity were assessed by comparing percentages of responses to increasing sucrose concentrations with a repeated-measure ANOVA, as well as average SRS values with a one-factor ANOVA. We applied an arcsin transformation of the data before applying ANOVA, and multiple comparisons were applied using a Bonferroni correction.

Results

Screening of ligands of the ASTA receptor. We aimed to perform a virtual screening to find non-peptidic ligands for the honey bee allatostatin A receptor (ASTA-R). With this purpose, we created a homology model of the receptor based on the structure of the human δ -opioid receptor³⁰, since no allatostatin receptor structures are yet available (see Methods). We used electrostatic probes on the area that corresponds to the typical orthosteric binding pocket of class A GPCRs to define possible requirements (a pharmacophore model) of putative ASTA-R ligands (Fig. 1).

We screened a subset of the ZINC database³² as described in the Methods section. The fact that we use a model based on an inactive receptor should favor identifying antagonists. Yet, because it is not known if any of the pharmacophoric features used is associated with agonism or antagonism, hits could be either agonists or antagonists. After visual inspection of the best 1000 ranked compounds, we selected 24 molecules for experimental testing (‘A compounds’, Sup. Table 1).

All 24 compounds were tested for their capacity to compete with ¹²⁵I-ASTA on HEK 293 cells transfected with the ASTA receptor (Fig. 2). While ASTA had an IC₅₀ in the nanomolar range (Fig. 2a), consistently with previous data⁶, only 3 of the tested compounds were able to compete in a dose-dependent manner, with low micromolar affinities: A8, A16 and A23 (Fig. 2b). These active molecules were used to optimize the ligand binding modes in the receptor model, and were selected for testing in vivo.

Modulation of behavioral manifestations of stress. We ran experiments to test the capacity of A8, A16 and A23 to act as a possible antagonists of ASTA-R in vivo, and thus to limit behavioral manifestations of the stress response. For this, we used the exposure to IPA (the main component of alarm pheromone) as the stress condition. Our previous work showed that exposure to IPA reduces both the learning performance and the probability of appetitive responses. We thus tested whether treating bees with either compound prior to exposure could reduce the impact of this stressor on behavior. First, bees were exposed to IPA following injections of the tested molecule, then submitted to a classical conditioning assay where they had to learn to respond to an odorant which was repeatedly delivered in association with a food reward. Two control groups injected with PBS: one was unstressed (exposed to oil only) and the other was exposed to IPA. We focused on A8 since neither A16 nor A23 appeared to have detectable effects in a preliminary experiment (Fig. S1). While, as expected, the stressed control PBS group displayed a marked decrease in learning as compared to its unstressed counterpart at the end of conditioning, the performance of A8-treated bees seemed to display a U-shape dose-dependent curve (trial \times dose effect: $F_{3,104} = 2.627$, $p = 0.0345$) (Fig. 3).

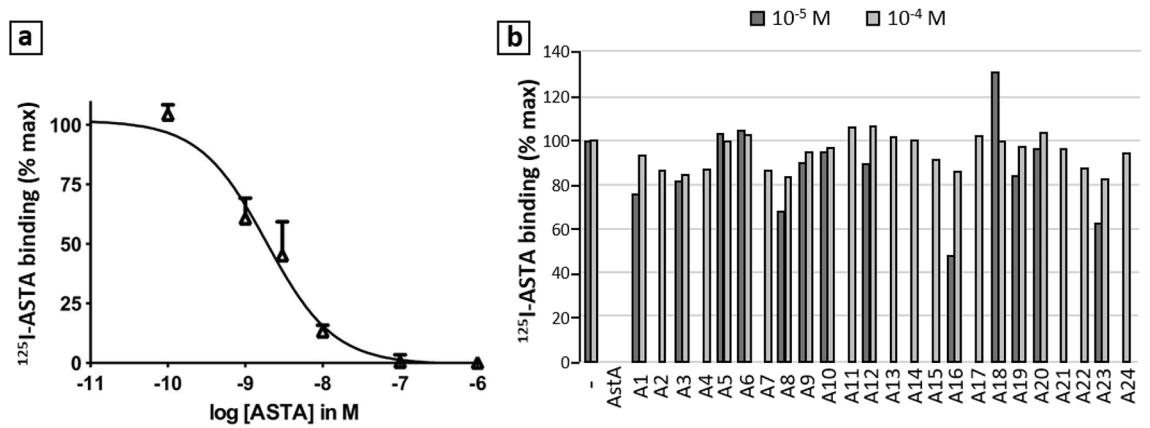


Figure 2. In vitro competitive binding assays for the A-series molecules. **(a)** Competition curve for the native ligand ASTA on HEK cells. **(b)** Results (% max) obtained with the 24 tested A molecules (positive control: ASTA 10⁻⁶ M). Only A8, A16 and A23 showed dose-dependent binding (3 replicates).

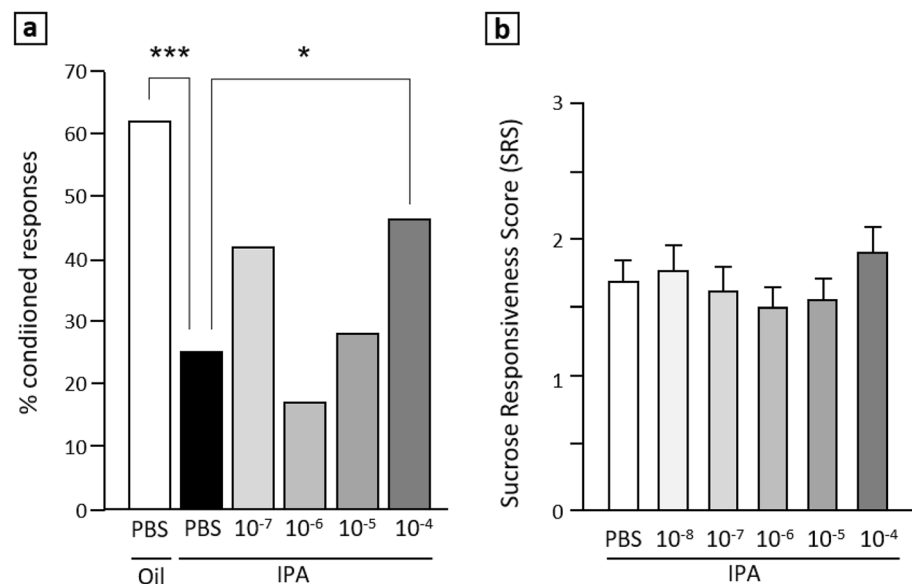


Figure 3. Effects of A8 on stressed bees. **(a)** Learning: proportions of individuals showing a conditioned response to the odorant paired with sucrose, at the end of the conditioning session (third trial). Bees were injected either with PBS or A8, then exposed to IPA or paraffin oil only (negative controls). While exposure to IPA significantly reduced learning performance in PBS-injected bees, this effect was restored by an injection of 10⁻⁴ M A8. *: $p < 0.025$; *** $p < 0.0005$ (PBS: $n = 100$; A8: $n = 47$ –99/group). **(b)** Sucrose responsiveness: mean sucrose responsiveness score values in bees injected with PBS or A8 before exposure to IPA. Even at the highest dose, A8 could not significantly increase SRS as compared to PBS controls (PBS: $n = 78$; A8: $n = 44$ –47/group) (2 replicates).

The learning performances of bees receiving the highest and lowest A8 doses did not differ from those of negative controls (unstressed bees receiving PBS) (10⁻⁷ M: $Z = 2.233$, $p = 0.0001$; 10⁻⁴ M: $Z = 2.025$, $p = 0.0048$). However, only 10⁻⁴ M doses performed better than that of stressed bees ($Z = 2.842$, $p = 0.0224$) (Fig. 3a). Thus, high doses of A8 could restore the learning performance of stressed bees at a level comparable to that of unstressed bees. We then focused on A8 for further experiments and to optimize the ligand binding modes in the receptor model.

In the same experiment, we compared the proportions of bees that had to be discarded due to a lack of proboscis extension reflex in response to 50% sucrose (the unconditioned stimulus used in the learning task). Indeed, exposure to IPA markedly increased this proportion in PBS-injected bees (IPA/PBS: 38.5%; Oil/PBS: 1.9%; $Z = 4.458$, $p < 0.001$), consistently with previous works, indicating a reduced motivation for food²⁴. However, this effect was significantly attenuated following treatment with A8 at 10⁻⁴ M (IPA/10⁻⁴: 23.4%, $Z = 2.249$, $p = 0.049$). Thus, A8 improved the probability to respond to 50% sucrose, a coarse measure of appetitive motivation. In order to explore further the action of A8 on sucrose responsiveness, we used a standard protocol designed to provide a more sensitive assessment of appetitive motivation through the calculation of individual sucrose

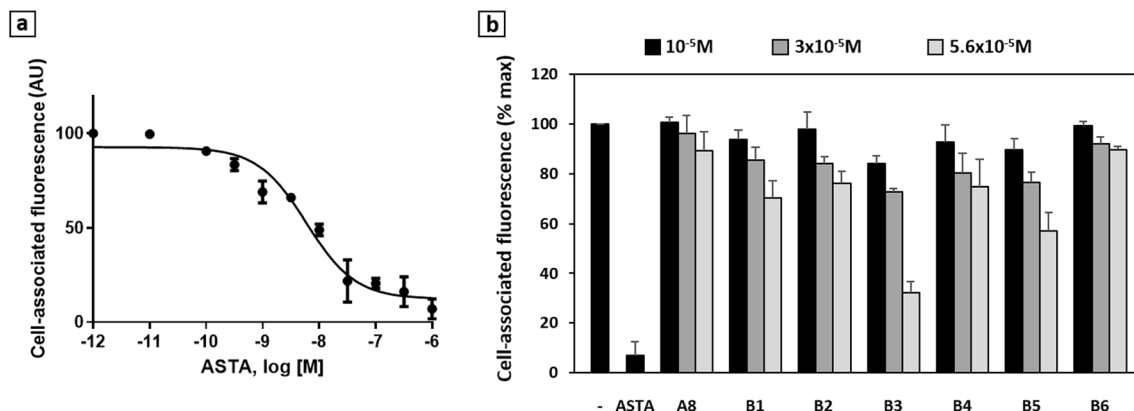


Figure 6. In vitro competitive binding assays for the B-series molecules. (a) Competition curve for the native ligand ASTA on HEK cells (4 replicates). (b) Results (% max) for the 6 tested B molecules, as compared with those of A8 and ASTA (10^{-6} M) (5 replicates).

Finally, intermediate amines 3a-b were coupled with acid derivatives 5a-c which were prepared in variable yields (60–95%) by reaction of thioglicolic acid with the corresponding phenylalkyl bromides 4a-c using NaOH as base, as previously described³³. This coupling reaction resulted troublesome, leading to low yields of amides B1–6 when using carbodiimide based coupling reagents. Finally, the best conditions for amine 3a were achieved the corresponding acid chloride derivatives of acids 5a-c and diisopropyl ethyl amine (DIPEA) as base, obtaining amides B1–3 in reasonably good yields (56–83%), whereas for amine 3b the best reaction conditions resulted using the uronium coupling reagent HATU along with carboxylic acids 5a-c and DIPEA as base, to afford the targeted compounds B4–6 in similar yields (50–83%). The structural identity of all compounds were determined by NMR spectroscopy and HRMS (see Supplementary Material).

Binding efficiency of new molecules in vitro. The ability of these new potential ligands to bind to the ASTA receptor was tested on HEK cells, using a competitive binding assay. Their capacity to compete with fluorescence-labeled ASTA was compared to that of A8 at the same concentrations, in order to test whether the ligand had been improved by some of the chemical modifications brought to the original molecule. In all 6 cases, the affinities were low, as indicated by IC_{50} values greater than 10^{-5} M. Only B3 and B5 present affinities that seem slightly improved as compared with that of A8, but still far below that of ASTA (Figs. 6 and S3).

Increased efficiency of new molecules as modulators of the stress response. The new selection of ligands was tested in vivo for their capacity to restore appetitive responses in stressed bees at various concentrations, using the same protocol as for compound A8. Here, the range of tested doses excluded 10^{-4} M, since we looked for significant effects that would be observable at lower doses than with A8. For the purpose of comparing the relative efficiencies of these molecules, all PBS-treated bees were pooled in a common control group, since no significant difference was found between the respective control groups ($F_{6,5305} = 0.764$; $p = 0.577$). The response trends over the range of sucrose concentrations can be visualized in Fig. S2. While overall, bees responded more often as sucrose got more concentrated ($F_{5,5305} = 513.30$; $p < 0.001$), their sensitivity was affected differently by the 6 tested molecules ($F_{6,1061} = 6.11$; $p < 0.001$). The proportions of responsive bees tended to increase after treatment with B2, B1 and B4, but without any obvious dose dependence. On the contrary, B3, B5 and B6 seemed to improve responsiveness to sucrose at higher doses. A repeated ANOVA on each dataset revealed a significant dose-dependent effect only for the two latter molecules (B5: $F_{4,340} = 4.06$; $p = 0.003$ B6: $F_{4,337} = 2.75$; $p = 0.029$).

For the purpose of comparison, we provide in Fig. 7 the mean sucrose responsiveness score values (SRS). As a mean to determine the efficient range of concentrations of B5 and B6, we ran multiple comparisons between individual doses and the PBS group. As a result, B5 induced a significant improvement of sucrose responsiveness at doses ranging from 10^{-7} to 10^{-5} M (10^{-7} : $F_{1,240} = 7.92$; $p = 0.005$; 10^{-6} : $F_{1,237} = 6.76$; $p = 0.010$; 10^{-5} : $F_{1,247} = 8.05$; $p = 0.005$), and B6 did so only at 10^{-5} M (10^{-5} : $F_{1,240} = 7.46$; $p = 0.007$). We further compared the effects of B5 and B6 at 10^{-4} M with those of A8 at the same concentration. The results, which have been included in Fig. 7 for the sake of comparison, show that neither B5 nor B6 could improve sucrose responsiveness at this high dose, contrary to A8 ($F_{1,267} = 9.64$; $p = 0.002$). Thus B5, and B6 to a lesser extent, proved efficient to reduce the effects of stress on appetitive motivation within intermediate ranges of concentrations, at lower doses than A8.

B5 and B6 compounds act as antagonists of ASTA signaling. Since B5 and B6 compounds counteract behavioural effects of stress, we hypothesized that they could do so by inhibiting the action of ASTA as a putative stress signal. Hence, we tested their capacity to modulate the action of ASTA on its receptor in transfected cells. Since the ASTA-R was shown to be coupled to the Gai subtype⁶, which decreases cAMP (cyclic adenosine monophosphate) production via adenylyl cyclase inhibition, we exposed cells to forskolin, which activates adenylyl cyclase and increases intracellular levels of cAMP, in the presence or absence of allatostatin and/or B5 or B6 compounds. As shown in Fig. 8, ASTA significantly decreased the forskolin-induced intracellular cAMP levels by $32.2 \pm 8.2\%$ ($p = 0.0045$), indicating that, upon activation by its ligand, ASTA-R was coupled

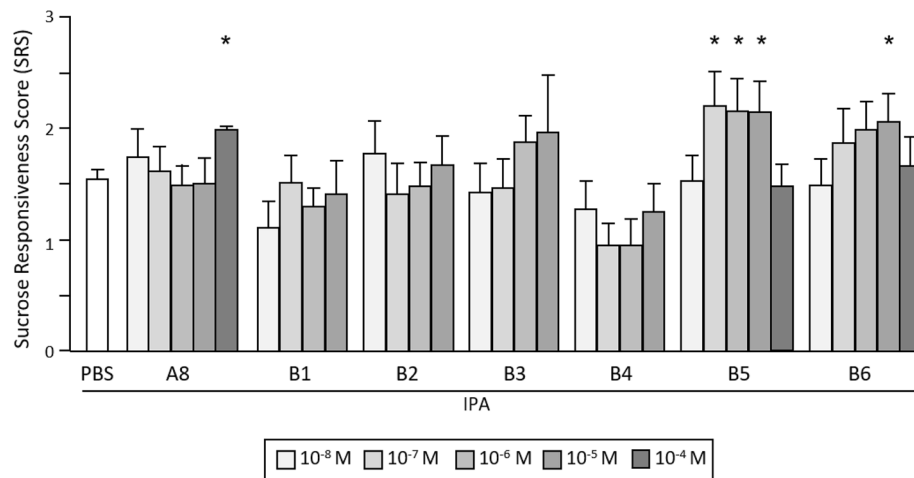


Figure 7. Compared effects of B-series molecules on sucrose responsiveness. Mean sucrose responsiveness score values in bees injected with PBS, A8, or either molecule of the B series (between 10^{-8} and 10^{-5} M), then exposed to IPA (2 replicates). Data from an additional experiment using injections of A8, B5 and B6 at 10^{-4} M have been included. Treatment with B5 or B6 significantly improved sucrose responsiveness, with a greater efficiency than A8, particularly for B5. *: $p < 0.05$ (PBS: $n = 186$; B compounds: 28–41/group).

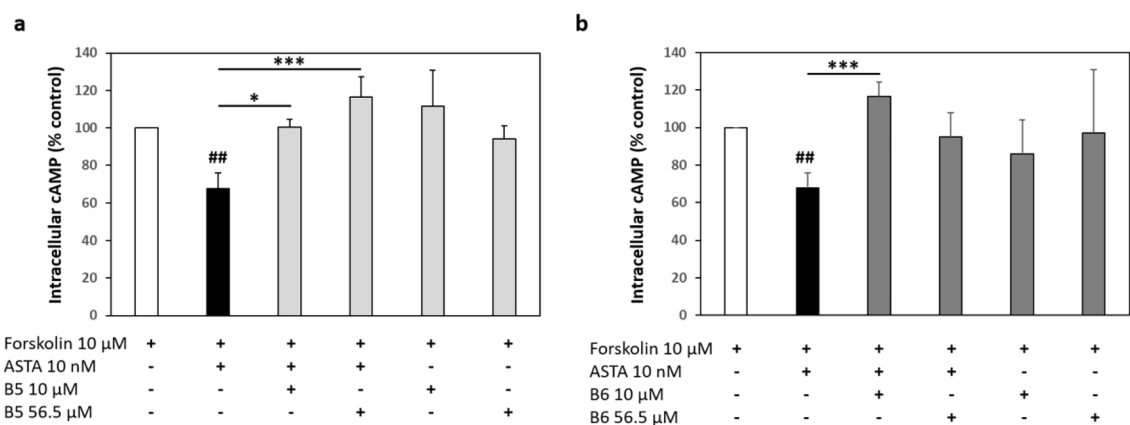


Figure 8. Effects of B5 and B6 compounds on ASTA signaling in vitro. Relative levels of forskolin-induced intracellular cAMP (expressed as percentages of control levels, i.e. with forskolin only). Treatment with ASTA significantly decreased cAMP levels, which was reversed when either B5 (a) or B6 (b) was added (albeit not significantly with 56.5 μM B6). #: $p < 0.01$ (vs. forskolin only); *: $p < 0.05$; ***: $p < 0.0005$ (vs. forskolin + ASTA) (at least 5 replicates per combination).

to Gai protein and inhibited adenylyl cyclase. In presence of B5 (Fig. 8A; 10 nM: $p = 0.013$, 56.5 μM: $p = 0.0002$) or B6 (Fig. 8B; 10 nM: $p = 0.0007$), this capacity for ASTA to inhibit adenylyl cyclase was significantly reduced (so that the cAMP production was similar to control levels. Importantly, in absence of ASTA, neither B5 or B6 alone (in absence of ASTA) could decrease the forskolin-induced intracellular cAMP levels when incubated in ASTA-R expressing cells. These results suggest that both B5 and B6 act as ASTA antagonists by interacting with ASTA-R.

Discussion

Bees are exposed to many biotic and abiotic stressors, which trigger behavioral and physiological responses through largely unknown signaling pathways. Here, we took advantage of the identified role of allatostatins in modulating behavioral responses to an ecologically-relevant stress: exposure to IPA, the main component of the sting alarm pheromone signaling potentially dangerous situations (e.g. predation). Here, a screening for potential ligands of the ASTA receptor led to identify one compound (A8) that proved efficient on behavioral measures of stress. Chemical synthesis of derivatives of this molecule enabled to increase this efficiency. To our knowledge, this is the first demonstration of a physiological effect of synthesized small-molecule ligand of a neuropeptide receptor in invertebrates. Previous work used comparable strategies to target diverse insect peptidergic pathways^{36–40} but we are unaware of published physiological or behavioral effects of the ligands identified in vitro.

Exposure to IPA triggers a series of behavioral changes that all relate to the recruitment of individuals for colony defense, on the expense of foraging: increased locomotor activity and aggressiveness^{14,15}, decreased sensitivity to noxious stimuli^{16,17}, reduced responsiveness to food^{17,18} and decreased performance in an appetitive learning task¹⁸. These behaviors are reminiscent of typical manifestations of stress in vertebrates. Injection of ASTA has similar effects on sucrose responsiveness and learning performance⁶, while it is not known yet whether ASTA recapitulates other behavioral manifestations of stress. Interestingly, in *Drosophila* ASTA signaling seems to respond to specific physiological or environmental conditions such as nutritional stress^{20–22}. Whether it participates more broadly in a more general stress response in that species is not established, but this is plausible since it promotes and coordinates the action of AKH (adipokinetic hormone) and DILPs (*Drosophila* insulin-like peptides), two signals involved in stress responses^{41,42}. Here, by showing that ligands of the ASTA receptor antagonize some effects of IPA exposure, our results provide additional support for a key regulating function of allatostatins (at least ASTA) in modulating stress responses. Based on the data from *Drosophila*, ASTA might be involved in an acute stress response involving the release of glucose (and possibly lipids) in the haemolymph²¹, thus providing rapidly mobilized energy sources to fight stress such as following exposure to IPA. As a consequence, bees would behave as if satiated, i.e. displaying low appetitive motivation for sucrose and decreased performance in appetitive learning. Consistently with this model, the capacity of the tested compounds to promote sucrose responsiveness and (at least for A8) re-establish learning performance in stressed bees, might be the consequence of limiting IPA-triggered glucose release. Since such molecules here could reverse the effects of IPA exposure, they appear to counteract that of ASTA. As they could also compete with ASTA in binding assays and inhibit its signaling through adenylyl cyclase, they appear to act as competitive antagonists of the ASTA receptor. Yet, their selectivity remains to be assessed, so that we cannot exclude that they act on the ASTC receptor and/or others, particularly given their relatively high concentration range of action.

Independently of their exact mechanisms of action, some of the compounds tested in this study could modulate different behavioral manifestations of stress, in a dose-dependent manner. In particular, the A8 compound proved to restore, at least partially, both the learning performance and the motivation for sucrose. Since the learning task is a standard appetitive assay using sucrose as a reward, in principle the effects on learning performance might be a mere consequence of changes in appetitive motivation (the higher the motivation, the higher the probability to learn). Yet, both actions appear to be largely independent. First, learning was assessed only in bees responding to 50% sucrose, thus ensuring a sufficient motivation in all trained bees. It was simply the capacity to reach this minimal level of motivation (before learning) that was modulated by A8. Second, when A8 significantly affected responsiveness to less concentrated sucrose, it did so by increasing it, which would rather predict decreased learning (bees with higher SRS values tend to learn less well, as their motivation is lower^{43,44}). Thus, A8 modulated learning performance in responding bees independently of its reducing action on responsiveness scores. Importantly, this dual effect is reminiscent of the situation in fruitflies, where blocking ASTA-expressing neurons could impair sugar-mediated appetitive learning without affecting innate sugar preference²³. However, a notable difference between the two species is that ASTA decreases sucrose responsiveness but promotes appetitive learning in flies, while it reduced both in bees¹⁹. Nevertheless, the effects of A8 thus mirror those triggered by IPA exposure¹⁸; however, they were obtained in the millimolar range (10^{-4} M), while ASTA could significantly impair learning already in the micromolar range (10^{-6} – 10^{-4} M)⁶. This limited efficiency advocated for the search of more efficient compounds.

As an assessment of in vivo effects of the chemically-synthesized derivatives of A8 (B molecules), we focused on SRS measurement as a rather quick way to screen several compounds at multiple doses. This approach enabled revealing a capacity for B5 and B6 to increase sucrose responsiveness, thus having more potent modulatory effects on appetitive motivation than A8. In addition, they displayed such biological activity at concentrations respectively 1000 and 10 times lower than for A8, thus in a range comparable to that of ASTA⁶. They thus appear as more potent modulators on the basis of this preliminary work. While further experiments will be necessary in the future to assess their effects on other behavioral parameters of the stress response, they are clearly (particularly B5) interesting candidate modulators of the bee stress response, through the inhibition of ASTA signaling. Which structural changes may explain this improvement? The substitution of the $-CF_3$ group on the phenyl ring, a common point between B5 and B6, appears to be a major factor of improvement, since no behavioral effect was detected using any fluorinated derivative (B1–3). In addition, a length of 2–3 carbon atoms for the chain connecting the phenyl rings seems optimal, since with a shorter chain B4 displayed no clear effect. Interestingly, B3, with a 3-carbon chain, was the only fluorinated compound showing a trend for a dose-dependent improvement of sucrose responsiveness. Likewise, only B3 and B5 had a slightly increased affinity for the receptor in our in vitro binding assay. However, these values remained low, and the substitution of the $-CF_3$ group had no clear effect on affinity, thus making difficult to relate chemical specificities, binding properties and physiological effects. There are several possible explanations for this discrepancy. The actual conformation of the receptor in vivo might be more favorable towards B5 binding, or the de-fluorinated compounds might show improved tissue penetration (and thus efficiency) due to a reduced hydrophobicity^{40,45}. Such hypotheses might also explain why A16 or A23 (which bears a fluorine group) failed to modulate learning in preliminary experiments when used as the same concentration as A8, despite rather similar affinities in vitro, although we cannot discard that they might be effective at different doses and/or might affect other behavioral parameters.

Earlier work suggested that the activation of ASTA-R might reduce cyclic AMP levels through coupling with Gi (consistently with our results own results) and/or Go proteins⁶, as for its closest mammalian homologue, GALR1^{46,47}. However, the protective effects of galanin under stressful conditions are due to its capacity to inhibit the hypothalamic–pituitary–adrenal through GALR1⁴⁸, while ASTA rather promotes stress-like responses. Thus, it seems that signaling through ASTA and galanin receptors modulate stress in opposite directions. Consistently, as discussed above the compounds appear to modulate sucrose responsiveness by acting as antagonists, while in mammals it is the activation of GAL receptors (most likely GALR1) by galanin that attenuates the activity

of midbrain reward circuits²⁴. Thus, despite conservation of some of their structural and functional features, ASTA and GAL receptors appear to modulate stress responses through different mechanisms. This conclusion supports the necessity to further explore the specificities of stress regulation in bees, and to develop specific strategies to improve their resilience. The present work is a first step in this novel direction, in contrast with most studies searching for ligands of insect receptors for pest control purposes [e.g.^{38,39}], and calls for further work to investigate whether the effects of other stressors on bee learning and/or sucrose responsiveness (e.g. parasites, pesticides^{48–51}) are mediated by the allatostatin system. Nevertheless, the present study shows that the search for synthetic compounds targeting specific bee receptors can prove effective, a strategy that can be extended to target other pathways as well.

Data availability

The datasets generated and analyzed during the current study are available from the corresponding authors on reasonable request.

Received: 9 March 2022; Accepted: 21 September 2022

Published online: 06 October 2022

References

- Gallai, N., Salles, J. M., Settele, J. & Vaissière, B. E. Economic valuation of the vulnerability of world agriculture confronted with pollinator decline. *Ecol. Econ.* **68**, 810–821 (2009).
- Goulson, D., Nicholls, E., Botías, C. & Rotheray, E. L. Bee declines driven by combined stress from parasites, pesticides, and lack of flowers. *Science* **347**, 1255957 (2015).
- Even, N., Devaud, J.-M. & Barron, A. General stress responses in the honey bee. *Insects* **3**(4), 1271–1298 (2012).
- McEwen, B. S. The brain is the central organ of stress and adaptation. *Neuroimage* **47**, 911–913 (2009).
- Liu, L., Yu, X., Meng, F., Guo, X. & Xu, B. Identification and characterization of a novel corticotropin-releasing hormone-binding protein (CRH-BP) gene from Chinese honeybee (*Apis cerana cerana*). *Arch. Insect Biochem. Physiol.* **78**(3), 161–175 (2011).
- Urlacher, E. *et al.* Honey bee allatostatins target galanin/somatostatin-like receptors and modulate learning: A conserved function?. *PLoS ONE* **11**(1), e0146248. <https://doi.org/10.1371/journal.pone.0146248> (2016).
- Schoofs, L., De Loof, A. & Van Hiel, M. B. Neuropeptides as regulators of behavior in insects. *Annu. Rev. Entomol.* **62**, 35–52. <https://doi.org/10.1080/01677063.2020.1839066> (2017).
- Nässel, D. R. & Zandawala, M. Recent advances in neuropeptide signaling in *Drosophila*, from genes to physiology and behavior. *Prog. Neurobiol.* **179**, 101607. <https://doi.org/10.1016/j.pneurobio.2019.02.003> (2019).
- Alcedo, J. & Prahlad, V. Neuromodulators: An essential part of survival. *J. Neurogenet.* **34**(3–4), 475–481. <https://doi.org/10.1080/01677063.2020.1839066> (2020).
- Rotzinger, S., Lovejoy, D. A. & Tan, L. A. Behavioral effects of neuropeptides in rodent models of depression and anxiety. *Peptides* **31**(4), 736–756. <https://doi.org/10.1016/j.peptides.2009.12.015> (2010).
- Schank, J. R., Ryabinin, A. E., Giardino, W. J., Ciccocioppo, R. & Heilig, M. Stress-related neuropeptides and addictive behaviors: beyond the usual suspects. *Neuron* **76**(1), 192–208. <https://doi.org/10.1016/j.neuron.2012.09.026> (2012).
- Holmes, A. & Picciotto, M. R. Galanin: A novel therapeutic target for depression, anxiety disorders and drug addiction?. *CNS Neurol. Disord. Drug Targets* **5**(2), 225–232 (2006).
- Free, J. B. *Pheromones of Social Bees* (Comstock Publishing Associates, 1987).
- Hunt, G. J. Flight and fight: A comparative view of the neurophysiology and genetics of honey bee defensive behavior. *J. Insect Physiol.* **53**, 399–410 (2007).
- Collins, A. M. & Blum, M. S. Alarm responses caused by newly identified compounds derived from the honeybee sting. *J. Chem. Ecol.* **9**, 57–65 (1983).
- Núñez, J., Almeida, L., Balderrama, N. & Giurfa, M. Alarm pheromone induces stress analgesia via an opioid system in the honeybee. *Physiol. Behav.* **63**, 75–80 (1998).
- Balderrama, N., Núñez, J., Guerrieri, F. & Giurfa, M. Different functions of two alarm substances in the honeybee. *J. Comp. Physiol. A Neuroethol. Sens. Neural. Behav. Physiol.* **188**, 485–491 (2002).
- Urlacher, E., Francés, B., Giurfa, M. & Devaud, J.-M. An alarm pheromone modulates appetitive olfactory learning in the honeybee (*Apis mellifera*). *Front. Behav. Neurosci.* **4**, 157 (2010).
- Urlacher, E., Devaud, J.-M. & Mercer, A. R. C-type allatostatins mimic stress-related effects of alarm pheromone on honey bee learning and memory recall. *PLoS ONE* **12**(3), e0174321. <https://doi.org/10.1371/journal.pone.0174321> (2017).
- Hergarden, A. C., Tayler, T. D. & Andersen, D. J. Allatostatin-A neurons inhibit feeding behavior in adult *Drosophila*. *PNAS* **109**(10), 3967–3972. <https://doi.org/10.1073/pnas.1200778109> (2012).
- Hentze, J. L., Carlsson, M. A., Kondo, S., Nässel, D. R. & Rewitz, K. F. The neuropeptide allatostatin A regulates metabolism and feeding decisions in *Drosophila*. *Sci. Rep.* **5**, 11680. <https://doi.org/10.1038/srep1168023> (2015).
- Chen, J. *et al.* Allatostatin A signalling in *drosophila* regulates feeding and sleep and is modulated by PDF. *PLoS Genet.* **12**(9), e1006346. <https://doi.org/10.1371/journal.pgen.1006346> (2016).
- Yamagata, N., Hiroi, M., Kondo, S., Abe, A. & Tanimoto, H. Suppression of dopamine neurons mediates reward. *PLoS Biol.* **14**(12), e1002586. <https://doi.org/10.1371/journal.pbio.1002586> (2016).
- Drolet, G. *et al.* Role of endogenous opioid system in the regulation of the stress response. *Prog. Neuropsychopharmacol. Biol. Psychiatry* **25**(4), 729–471. [https://doi.org/10.1016/s0278-5846\(01\)00161-0](https://doi.org/10.1016/s0278-5846(01)00161-0) (2001).
- Picciotto, M. R., Brabant, C., Einstein, E. B., Kamens, H. M. & Neugebauer, N. M. Effects of galanin on monoaminergic systems and HPA axis: Potential mechanisms underlying the effects of galanin on addiction- and stress-related behaviors. *Brain Res.* **1314C**, 206. <https://doi.org/10.1016/j.brainres.2009.08.033> (2010).
- Kuteeva, E. *et al.* Differential role of galanin receptors in the regulation of depression-like behavior and monoamine/stress-related genes at the cell body level. *Neuropsychopharmacology* **33**(11), 2573–2585. <https://doi.org/10.1038/sj.npp.1301660> (2008).
- Kozlovsky, N., Matar, M. A., Kaplan, Z., Zohar, J. & Cohen, H. The role of the galaninergic system in modulating stress-related responses in an animal model of posttraumatic stress disorder. *Biol. Psychiatry* **65**(5), 383–391. <https://doi.org/10.1016/j.biopsych.2008.10.034> (2009).
- Browne, C. A., Falcon, E., Robinson, S. A., Berton, O. & Lucki, I. Reversal of stress-induced social interaction deficits by buprenorphine. *Int. J. Neuropsychopharmacol.* **21**(2), 164–174. <https://doi.org/10.1093/ijnp/pyx079> (2018).
- Marti-Renom, M. A. *et al.* Comparative protein structure modeling of genes and genomes. *Annu. Rev. Biophys. Biomol. Struct.* **29**, 291–325 (2000).
- Fenalti, G. P. *et al.* Molecular control of delta-opioid receptor signalling. *Nature* **506**(7487), 191–196 (2014).

31. Matsoukas, M. T. *et al.* Identification of small-molecule inhibitors of calcineurin-NFATc signaling that mimic the PxIxIT motif of calcineurin binding partners. *Sci. Signal.* **8**(382), ra63 (2015).
32. Irwin, J. J., Sterling, T., Mysinger, M. M., Bolstad, E. S. & Coleman, R. G. ZINC: A free tool to discover chemistry for biology. *J. Chem. Inf. Model.* **52**(7), 1757–1768. <https://doi.org/10.1021/acs.jcim.0c00675> (2012).
33. Ning, X. *et al.* Design, synthesis, and biological evaluation of (*E*)-3,4-dihydroxystyryl aralkyl sulfones and sulfoxides as novel multifunctional neuroprotective agents. *J. Med. Chem.* **57**, 4302–4312 (2014).
34. Zarudnitskii, E. V., Ivanov, V. V., Yurchenko, A. A., Pinchuk, A. M. & Tolmachev, A. A. C-Phosphorylation of 1,2,4-triazoles with phosphorus(III) halides. Synthesis of 4,5-dihydrobenzo[e][1,2,4]triazolo[5,1-c][1,4,2]diazaphosphinine derivatives. *Heteroatom. Chem.* **13**, 146–152 (2002).
35. Kommu, N., Ghule, V. D., Kumar, A. S. & Sahoo, A. K. Triazole-substituted nitroarene derivatives: Synthesis, characterization and energetic studies. *Chem. Asian J.* **9**, 166–178 (2014).
36. Sullivan, R. E. & Newcomb, R. W. Structure function analysis of an arthropod peptide hormone: Proctolin and synthetic analogues compared on the cockroach hindgut receptor. *Peptides* **3**(3), 337–344. [https://doi.org/10.1016/0196-9781\(82\)90096-1](https://doi.org/10.1016/0196-9781(82)90096-1) (1982).
37. Poels, J. *et al.* Substitution of conserved glycine residue by alanine in natural and synthetic neuropeptide ligands causes partial agonism at the stomoxytachykinin receptor. *J. Neurochem.* **90**(2), 472–478. <https://doi.org/10.1111/j.1471-4159.2004.02506.x> (2004).
38. Yoon, Y. K. *et al.* Pyrazolodiazepine derivatives with agonist activity toward *Drosophila* RYamide receptor. *Bioorg. Med. Chem. Lett.* **26**(20), 5116–5118. <https://doi.org/10.1016/j.bmcl.2016.08.039> (2016).
39. Wahedi, A., Gäde, G. & Paluzzi, J. P. Insight into mosquito GnRH-related neuropeptide receptor specificity revealed through analysis of naturally occurring and synthetic analogs of this neuropeptide family. *Front. Endocrinol.* **10**, 74. <https://doi.org/10.3389/fendo.2019.00742> (2019).
40. Wang, M. *et al.* 3D-QSAR based optimization of insect neuropeptide allatostatin analogs. *Bioorg. Med. Chem. Lett.* **29**, 890–895 (2019).
41. Nelson, J. M., Saunders, C. J. & Johnson, E. C. The intrinsic nutrient sensing adipokinetic hormone producing cells function in modulation of metabolism, activity, and stress. *Int. J. Mol. Sci.* **22**(14), 7515. <https://doi.org/10.3390/ijms22147515> (2021).
42. Gruntenko, N. E. & Rauschenbach, I. Y. The role of insulin signalling in the endocrine stress response in *Drosophila melanogaster*: A mini-review. *Gen. Comp. Endocrinol.* **258**, 134–139 (2018).
43. Scheiner, R., Page, R. E. Jr. & Erber, J. The effects of genotype, foraging role, and sucrose responsiveness on the tactile learning performance of honey bees (*Apis mellifera* L.). *Neurobiol. Learn. Mem.* **76**, 138–150 (2001).
44. Scheiner, R., Page, R. E. Jr. & Erber, J. Responsiveness to sucrose affects tactile and olfactory learning in preforaging honey bees of two genetic strains. *Behav. Brain Res.* **120**, 67–73 (2001).
45. Robalo, J. R., Huhmann, S., Kokschi, B. & Verde, A. V. The multiple origins of the hydrophobicity of fluorinated apolar aminoacids. *Chem* **3**, 881–897. <https://doi.org/10.1016/j.chempr.2017.09.012> (2017).
46. Nishibori, M., Oishi, R., Itoh, Y. & Saeki, K. Galanin inhibits noradrenaline-induced accumulation of cyclic AMP in the rat cerebral cortex. *J. Neurochem.* **51**, 1953–1955 (1988).
47. Lang, R., Gundlach, A. L. & Kofler, B. The galanin peptide family: Receptor pharmacology, pleiotropic biological actions, and implications in health and disease. *Pharmacol. Ther.* **115**, 177–207 (2007).
48. Mitsukawa, K., Lu, X. & Bartfai, T. Bidirectional regulation of stress responses by galanin in mice: Involvement of galanin receptor subtype 1. *Neuroscience* **160**, 837–846 (2009).
49. Frost, E. H., Shutler, D. & Hillier, N. K. Effects of fluvalinate on honey bee learning, memory, responsiveness to sucrose, and survival. *J. Exp. Biol.* <https://doi.org/10.1242/jeb.086538> (2013).
50. Piironen, S. & Goulson, D. Chronic neonicotinoid pesticide exposure and parasite stress differentially affects learning in honeybees and bumblebees. *Proc. Biol. Sci.* **283**(1828), 20160246. <https://doi.org/10.1098/rspb.2016.0246> (2016).
51. Gao, J. *et al.* *Tropilaelaps mercedesae* parasitism changes behavior and gene expression in honey bee workers. *PLoS Pathog.* **17**(7), e1009684. <https://doi.org/10.1371/journal.ppat.1009684> (2021).

Acknowledgements

ADM, FB and RA acknowledge the financial support from the Spanish Ministry of Economy and Innovation with FEDER funds (projects CTQ2016-75363-R and PID2019-106403RB-I00). JMD thanks Lucie Hotier and Olivier Fernandez for the maintenance of honey bee colonies, and acknowledges the financial support from the French Research Agency (ANR-13-ADAP-0002-01).

Author contributions

V.G., D.F., F.B., R.A., A.C. and J.M.D. designed and supervised the study. A.S.M., V.G., M.T.M., L.P.B., A.C. and J.M.D. performed experiments. V.G., F.B., R.A., A.C. and J.M.D. wrote the main manuscript text and prepared the figures.

Competing interests

The authors declare no competing interests.

Additional information

Supplementary Information The online version contains supplementary material available at <https://doi.org/10.1038/s41598-022-20978-y>.

Correspondence and requests for materials should be addressed to F.B., A.C. or J.-M.D.

Reprints and permissions information is available at www.nature.com/reprints.

Publisher's note Springer Nature remains neutral with regard to jurisdictional claims in published maps and institutional affiliations.



Open Access This article is licensed under a Creative Commons Attribution 4.0 International License, which permits use, sharing, adaptation, distribution and reproduction in any medium or format, as long as you give appropriate credit to the original author(s) and the source, provide a link to the Creative Commons licence, and indicate if changes were made. The images or other third party material in this article are included in the article's Creative Commons licence, unless indicated otherwise in a credit line to the material. If material is not included in the article's Creative Commons licence and your intended use is not permitted by statutory regulation or exceeds the permitted use, you will need to obtain permission directly from the copyright holder. To view a copy of this licence, visit <http://creativecommons.org/licenses/by/4.0/>.

© The Author(s) 2022